Arab J Sci Eng (2015) 40:2085–2093
DOI 10.1007/s13369-015-1680-3

RESEARCH ARTICLE - PHYSICS

# Effects of Inhibitor on PbS Thin Films Obtained by Chemical Bath Deposition

**Barış Altıokka**[1]

Received: 14 December 2014 / Accepted: 23 April 2015 / Published online: 1 May 2015


**Abstract** Thin films of polycrystalline lead sulfide (PbS) have been deposited on glass substrates by chemical bath deposition at 20 ± 1 °C in alkaline solutions. Aqueous solutions of lead nitrate ($Pb(NO_3)_2$), potassium hydroxide (NaOH), thiourea ($CS(NH_2)_2$) and sodium thiosulfate ($Na_2S_2O_3$) were used together for the first time to obtain thin films of PbS. The chemical kinetics was investigated according to the amounts of $Pb^{2+}$ concentrations measured by atomic absorption spectroscopy during the precipitation of PbS. It was found that sodium thiosulfate had an inhibitor effect for alkaline solutions. The structures of the films were characterized by X-ray diffractometer and showed that all the films had a galena-type cubic structure. The morphological characteristics of the PbS thin films were studied by scanning electron microscope and revealed that when the $Na_2S_2O_3$ compound was used, the shape of the nanoparticles changed from the polymorphic form to the pyramidal form and pinhole-free PbS thin films could be produced.

**Keywords** Chemical bath deposition · Lead sulfide · Inhibitor · Thin film

## 1 Introduction

In the last few years, nanocrystalline thin films have been investigated due to their various applications [1]. One of these thin films is lead sulfide which is an important narrow-band IV–VI compound semiconductor material [2]. Due to its unique properties, it is mostly utilized as an infrared sensor and for mid-infrared lasers [3]. In addition to these devices, PbS is widely used for solar absorbers, optical switches, heavy metal concentration monitoring, electrochemical sensors for hydrogen sulfide ($H_2S$), semiconductor active layers in common-gated thin film transistors [4] and decorative coatings [5].

The electrical and optical characteristics of grain boundary regions are altered by exposure to impurities, diffusion and field effects. Stoichiometric excess of lead in PbS (bulk) imparts n-type character, whereas deficient lead makes it p-type [6]. PbS has small direct optical band gap energy of 0.41 eV for bulk at room temperature [7] and relatively large bulk exciton Bohr radius (18 nm) [4]. PbS forms in galena structure which is a lead sulfide mineral with a chemical composition of PbS [8].

There are several methods to deposit PbS thin films. Some of the methods require high temperature such as spray pyrolysis (SP), chemical vapor deposition (CVD) and thermal evaporation (TE). On the other hand, hydrothermal, solvothermal and chemical bath deposition (CBD) generally require lower temperatures and allow synthesizing of PbS thin films of a good quality [9]. Among these methods, the CBD has many advantages such as being a low-cost method and easy to handle, and allowing large area deposition of highly homogeneous films [10]. In the CBD method, successive absorption and reaction take place on the surface of substrate in aqueous solution containing $Pb^{2+}$ and $S^{2-}$ [11]. If aqueous solution of lead nitrate, thiourea and sodium hydroxide is used, the reaction process for forming PbS films is considered as follows [12].

$$Pb(NO_3)_2 + NaOH \rightarrow Pb(OH)_2 + 2NaNO_3 \quad (1)$$

$$Pb(OH)_2 + 4NaOH \rightarrow Na_4Pb(OH)_6 \quad (2)$$

✉ Barış Altıokka
baltiokka@gmail.com

[1] Bilecik Vocational School of Higher Education, Bilecik Şeyh Edebali University, Bilecik 11210, Turkey

**Table 1** The summary of the deposition conditions and final concentrations of chemical compounds

| Experiments | $Pb(NO_3)_2$ (M) | NaOH (M) | $Na_2S_2O_3$ (M) | $CS(NH_2)_2$ (M) | Temperature (°C) | Deposition time (min) |
|---|---|---|---|---|---|---|
| Run1 | 0.0089 | 0.146 | 0 | 0.051 | 20 ± 1 | 50 |
| Run2 | 0.0089 | 0.146 | 0.0034 | 0.051 | 20 ± 1 | 90 |
| Run3 | 0.0089 | 0.146 | 0.0068 | 0.051 | 20 ± 1 | 125 |
| Run4 | 0.0089 | 0.146 | 0.0102 | 0.051 | 20 ± 1 | 160 |
| Run5 | 0.0089 | 0.146 | 0.0136 | 0.051 | 20 ± 1 | 230 |

$$Na_4Pb(OH)6 \rightarrow 4Na^+ + HPbO_2^- + 3OH + H_2O \quad (3)$$

$$CS(NH_2)_2 + OH^- \rightarrow CH_2N_2 + H_2O + SH^- \quad (4)$$

$$HPbO_2^- + OH^- \rightarrow PbS_{(solid)} + 2OH^- \quad (5)$$

There are many studies on chemically deposited PbS thin films carried by using sodium thiosulfate [13–15], but all of the depositions of PbS in the mentioned studies were carried out in acidic bath since sodium thiosulfate decomposes only in acidic medium [16]. However, there is no study in the literature on CBD of PbS carried by using $Pb(NO_3)_2$, $CS(NH_2)_2$, NaOH and $Na_2S_2O_3$ together. It was concluded in one study [17] that reaction rate prevented pinhole formation of PbS thin films but film morphology and pinhole formation were investigated at relatively high magnification (10,000×) of surface images. In recent studies [6,7,10,17], it was reported that pinhole-free and void-free PbS thin films could be obtained by CBD but high-magnification (10,000–20,000×) surface images were investigated in the mentioned studies. However, pinholes and voids may not be observed on high magnification of surface images but they may be observed on relatively low-magnification surface images. In the literature, relatively low-magnification surface images of PbS films were not investigated. However, poor growth regions, pinholes and voids allow shunt path in the bilayer and multilayer film devices [18].

In this work, $Pb(NO_3)_2$, $CS(NH_2)_2$, NaOH and $Na_2S_2O_3$ aqueous solutions were used together for deposition of PbS by CBD for the first time. It was found that $Na_2S_2O_3$ had an inhibitor effect for this bath condition. The reaction kinetics was investigated according to $Pb^{2+}$ concentrations in the final solutions during the depositions. It was determined that reaction rate had a great effect on crystallization and film morphology. The structures of the films were studied by using X-ray diffractometer (XRD) patterns. When the observed reaction rate constant was decreased from 62 up to 23 $L^{1.67}\,min^{-1}\,mol^{-1.67}$, the peak intensities increased directly proportional. The film morphologies were investigated at both high (30,000×) and low magnification (100×) of SEM images. Pinholes and voids were not observed on high magnification of surface image of the PbS thin film obtained by using only $Pb(NO_3)_2$, $CS(NH_2)_2$ and NaOH. When low magnification of surface image of this film was analyzed, it was observed that there were many pinholes and voids. When $Na_2S_2O_3$ was incorporated into final solutions, very interesting results were observed at high- and low-magnification surface images, for example the shape of crystal particles shifted from the polymorphic form to pyramidal form and pinholes and voids were not observed on surface images.

## 2 Experimental Details

The PbS thin films have been deposited on glass substrates by CBD. Before the deposition, both deposition bath and the glass substrates were rinsed with 10 % (w/w) hydrochloric acid and deionized water, respectively. Thereafter, the deposition bath and the glass substrates were left to dry at room temperature.

Experiments were grouped into five groups named as run1, run2, run3, run4 and run5. In a previous detailed study [19], in order to obtain compact and dense PbS film, the $Pb(NO_3)_2$, NaOH and $CS(NH_2)_2$were used as 0.0089, 0.146 and 0.051 M in final solution, respectively. Therefore, these concentrations were chosen in all experiments in the presence of different $Na_2S_2O_3$concentrations. The deposition conditions are summarized in Table 1. In the experiments, the chemical aqueous solutions of $Pb(NO_3)_2$, NaOH, $Na_2S_2O_3$ and $CS(NH_2)_2$ were added to the deposition bath in order. All the experiments were carried out at a constant temperature of 20 ± 1°C. The depositions were completed in various deposition times according to the $Pb^{2+}$ concentration which is given in Table 1.

The thicknesses of PbS thin films were found to be approximately 700 nm by applying the gravimetric method.

pHs of the final solutions were measured by HANNA HI 83141 pH meter. $Pb^{2+}$ concentrations in final solutions have been measured by a GBC 933AA atomic absorption spectroscopy (AAS) during the depositions. The structures of the films were studied by a PANalytical Empyrean XRD. Diffraction patterns of the films were recorded as a function of $2\theta$ angle. Morphologic characterizations of the films were performed without coated by a Zeiss supra 40VP SEM.

## 3 Results and Discussion

### 3.1 The Reaction Kinetics

Figure 1 shows the time dependence of $Pb^{2+}$ concentrations as measured by AAS during the depositions at different concentrations of sodium thiosulfate. After some time, the $Pb^{2+}$ concentrations decreased sharply indicating that the reaction of $Pb^{2+}$ + $S^{2-}$ is an autocatalytic reaction. This situation indicates that the reaction of $Pb^{2+}$ + $S^{2-}$ is an autocatalytic reaction. Besides, it is seen from the Fig. 1. that when the $Na_2S_2O_3$ was used in the depositions, the decrease in $Pb^{2+}$ concentrations slowed down. Thus, it can be said that $Na_2S_2O_3$ has an inhibitor effect in CBD of PbS for alkaline solution. It was reported that using an inhibitor in CBD of PbS increased the film quality [17].

It was seen in Table 1 that $Pb^{2+}$ ion is the limiting reactant to obtain PbS. The chemical reaction of $Pb^{2+}$ + $S^{2-}$ without an inhibitor is stated as follows:

$$A + B \xrightarrow{k_1} R \tag{6}$$

where $A$ is the $Pb^{2+}$, $B$ is the $S^{2-}$, $R$ is the solid PbS, and $k_1$ is the reaction rate constant. It was reported from Ref. [3] that the formed PbS particles in final solution accelerated the precipitation of PbS. Therefore the reaction between $Pb^{2+}$ and $S^{2-}$ was an autocatalytic reaction. Under this condition, the rate expression is written as [20].

$$\left(-\frac{dC_A}{dt}\right)_1 = k_1 C_R^r C_A^a C_B^b \tag{7}$$

where $C_R = C_{A0} - C_A$ is the concentration of PbS particles. It was reported that the values of reaction order $r$, $a$ and $b$ were 2/3, 1 and 1, respectively [20].

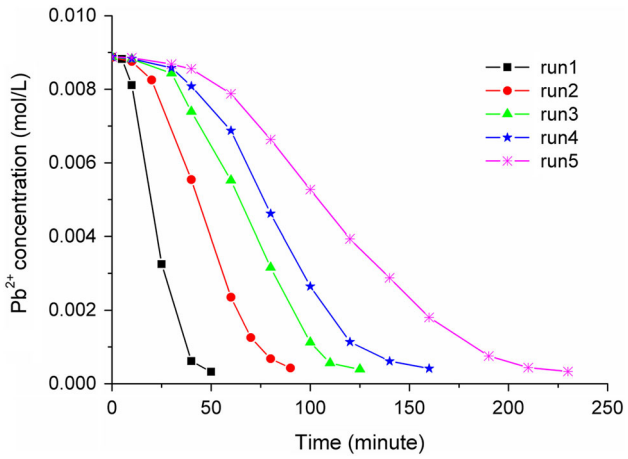


**Fig. 1** $Pb^{2+}$ concentrations, measured by atomic absorption spectroscopy, versus time

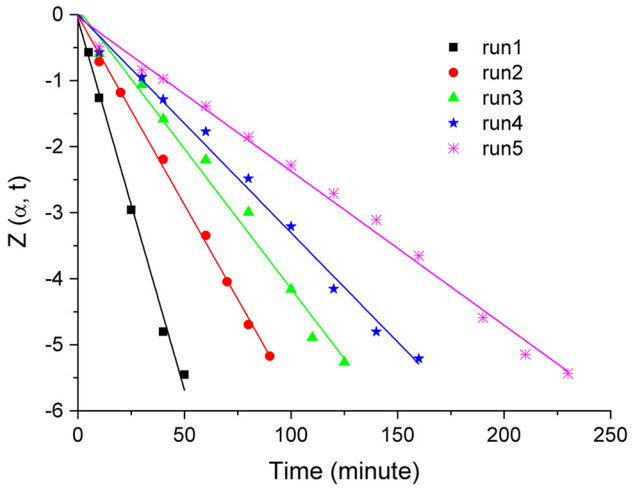


**Fig. 2** $Z(\alpha, t)$ versus time, the slopes calculated from left side of Eq. 12 divided $t$

When an inhibitor is used in the deposition, the reaction mechanism is written as seen in Eq. 8 [17].

$$A + B + C \xrightarrow{k_2} R + C \tag{8}$$

where $C$ is the inhibitor. Thus the rate expression in the presence of an inhibitor can be written as seen in Eq. 9.

$$\left(-\frac{dC_A}{dt}\right)_2 = k_2 C_C^c C_R^{2/3} C_A C_B \tag{9}$$

where $C_C$ is the concentration of the inhibitor, and $c$ is the reaction order. In this study, $C_C$ is the concentration of $Na_2S_2O_3$ and its value is constant because thiosulphate decomposes only at pH < 4.0 [16]. In this work, pHs of the final solutions were measured to be about 12.2. In this case, a reaction is both autocatalytic and includes an inhibitor, and the total rate expression is written as:

$$\left(-\frac{dC_A}{dt}\right)_{\text{total}} = k_{\text{obs}} C_R^{2/3} C_A C_B \tag{10}$$

where $k_{\text{obs}}$ is the observed reaction rate constant and it is equal to $k_1 + k_2 C_C^c$. The integrated form of Eq. 10 has been given by Ref. [20] in Eq.11.

$$Z(\alpha, t) = \frac{1}{2} \ln \frac{(1-(1-\alpha)^{1/3})^3}{\alpha} - \frac{1}{2\beta^{2/3}} \ln \frac{(\beta^{1/3} - (1-\alpha)^{1/3})^3}{\beta - (1-\alpha)} - \sqrt{3}\,\text{arctg}\frac{2(1-\alpha)^{1/3}+1}{\sqrt{3}}$$

**Table 2** The values of observed reaction rate constant at different sodium thiosulfate concentrations

| Experiment | Run1 | Run2 | Run3 | Run4 | Run5 |
|---|---|---|---|---|---|
| $C_C$ (mol L$^{-}$1) | 0 | 0.0034 | 0.0068 | 0.0102 | 0.0136 |
| $k_{obs.}$ $\left(L^{1.67}\,min^{-1}\,mol^{-1.67}\right)$ | 62.05 | 31.55 | 22.91 | 16.76 | 11.81 |

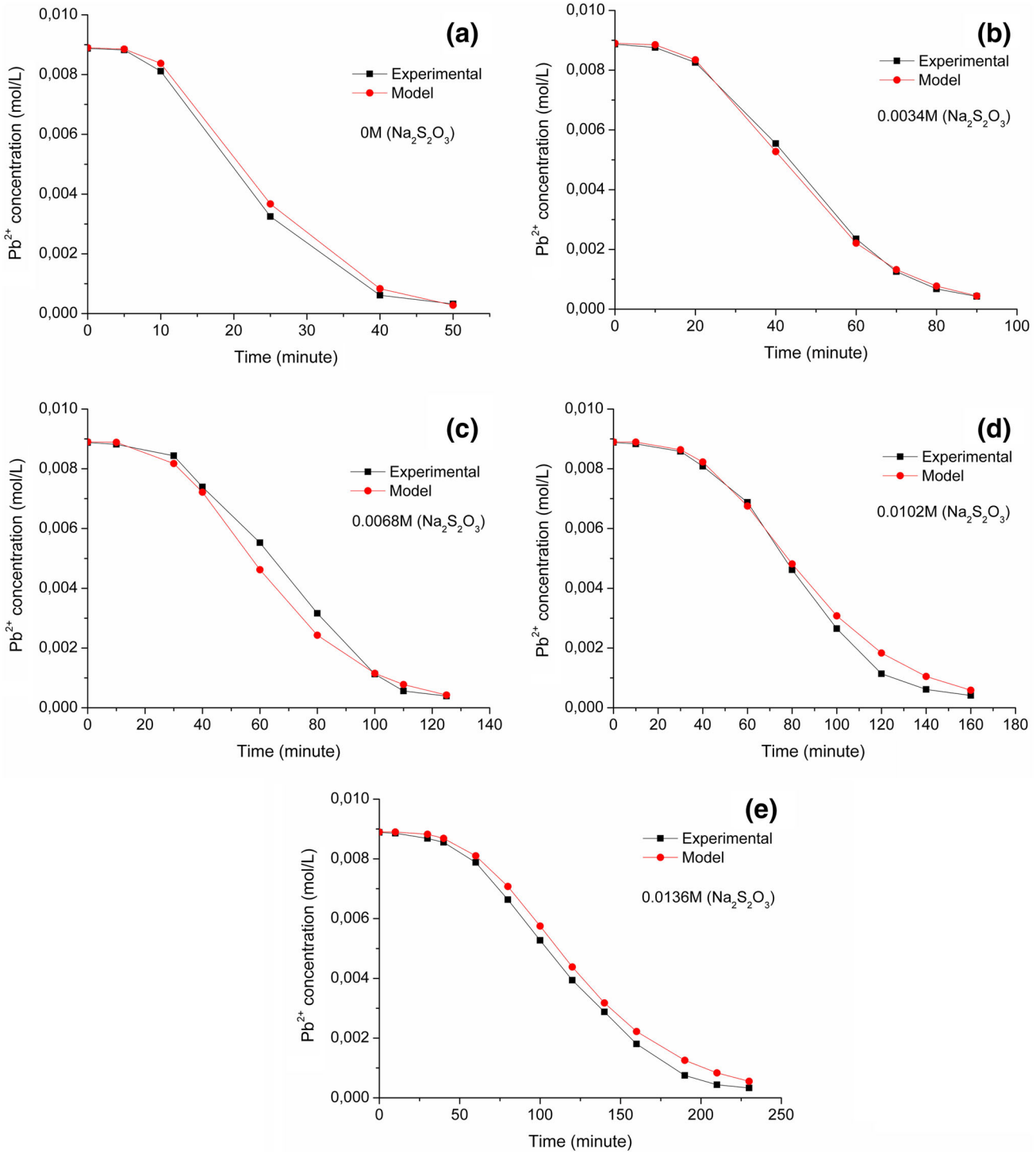


**Fig. 3** Comparison of the kinetics model with experimental data for $Na_2S_2O_3$ with different concentrations: **a** 0, **b** 0.0034 M, **c** 0.0068 M, **d** 0.0102 M and **e** 0.0136 M

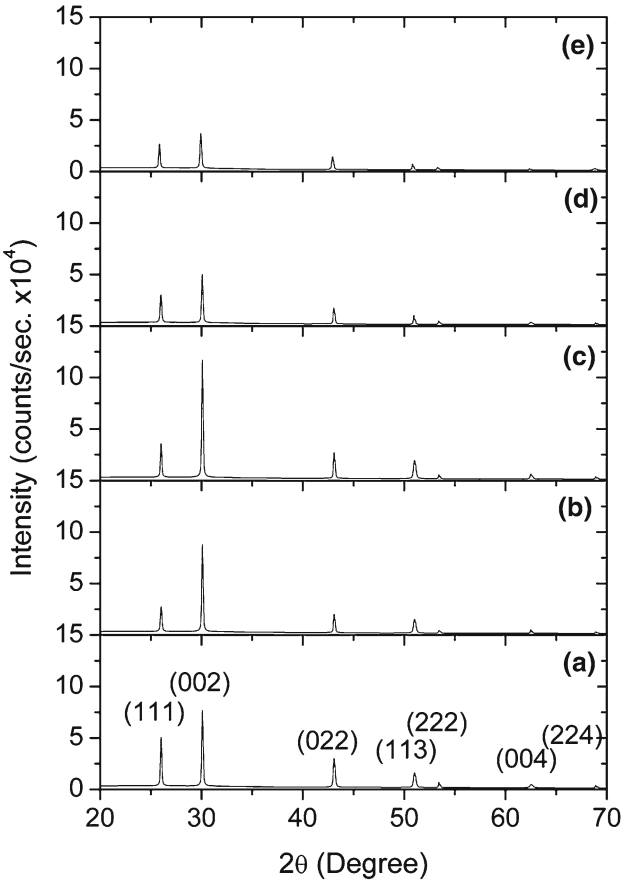


**Fig. 4** The XRD patterns of the PbS thin films deposited at various $Na_2S_2O_3$ concentration of **a** 0 M, **b** 0.0034 M, **c** 0.0068 M, **d** 0.0102 M and **e** 0.0136 M

$$+\frac{\sqrt{3}}{\beta^{2/3}}\text{arctg}\frac{2(1-\alpha)^{1/3}+\beta^{1/3}}{\beta^{2/3}\sqrt{3}} -\frac{\sqrt{3}(1-\beta^{2/3})}{\beta^{2/3}}\text{arctg}\frac{1}{3}=C_{A0}^{5/3}(1-\beta)k_{\text{obs.}}t \quad (11)$$

where $\alpha = C_A/C_{A0}$ and $\beta = C_{B0}/C_{A0}$. A graphic representation of Eq. 11 in the coordinates $Z(\alpha, t)$ vs. t is a straight line which is shown in Fig. 2. The slopes of this straight lines are equal to the $C_{A0}^{5/3}(1-\beta)\,k_{\text{obs.}}$, where the values of $C_{A0}$ and $\beta$ are constant. Thus $k_{\text{obs.}}$ can be obtained easily.

The values of the observed reaction rate constants are given in Table 2. When the concentration of sodium thiosulfate is zero, the $k_{\text{obs.}}$ is equal to the $k_1$. In this study, the value of $k_1$ was calculated as $62.5\,L^{1.67}\,min^{-1}\,mol^{-1.67}$. In a previous study, $k_1$ was calculated as $60.5\,L^{1.67}\,min^{-1}mol^{-1.67}$ [17].

The values of $k_2$ and reaction order $c$ were calculated as $-236\,L^{1.67}\,min^{-1}mol^{-1.67}$ and 0.36, respectively. In a previous study, in which sodium sulfite was used as an inhibitor, the values of $k_2$ and $c$ were calculated as $-92.5\,L^{1.67}\,min^{-1}\,mol^{-1.67}$ and 0.1, respectively [17]. These results show that sodium thiosulfate is a weaker inhibitor than sodium sulfate for CBD of PbS.

The measured $Pb^{2+}$ concentrations by AAS and theoretical $Pb^{2+}$ concentrations, which are calculated from the left side of the Eq. 11, are shown in Fig. 3.

The theoretical and the measured results are nearly same. These results are acceptable.

### 3.2 Structural Properties of PbS Thin Films

The XRD patterns of the PbS thin films are shown in Fig. 4. All XRD patterns show three intense peaks at around $2\theta$ = 26.00°, 30.00° and 43.06°. All of these peaks were related to the galena-type cubic structure of PbS which matched well with the ASTM card no (98-060-0243).

The preferred crystallographic orientations of all films are (002). It is also seen from the XRD patterns that the ratio of intensities of the (002) peak to the (111) peak of the films obtained in run1 to run5 is 1.52, 3.04, 3.26, 1.66 and 1.39, respectively. When the concentration of the $Na_2S_2O_3$in the final solution was gradually increased up to 0.0068 M, then the intensities of (002) peak of the obtained films gradually increased. On the other hand, when the concentration of the $Na_2S_2O_3$in the final solution was more than 0.0068 M, the intensities of (002) peak of the films decreased.

The crystallite sizes of the PbS thin films were calculated by applying Scherrer formula;

$$cs = \frac{K\lambda}{B\cos\theta} \quad (12)$$

where $cs$ is the crystallite size, $K$ is the constant, $\lambda$ is the wavelength of X-ray radiation (1.54 Å), $B$ is the full width at the half maximum peak height, and $\theta$ is the Bragg's angle [7, 11, 17, 21–31]. The calculated crystallite sizes of the PbS thin films are given in Table 3. The average crystallite size of the

**Table 3** The calculated crystallite sizes of the obtained PbS thin films

| Experiments | cs (nm) (111) | cs (nm) (002) | cs (nm) (022) | cs (nm) (113) | Average cs (nm) |
|---|---|---|---|---|---|
| Run1 | 83.0 | 83.6 | 68.9 | 51.0 | 71.6 |
| Run2 | 65.9 | 83.6 | 86.7 | 51.0 | 71.8 |
| Run3 | 83.0 | 83.6 | 86.7 | 51.0 | 76.1 |
| Run4 | 65.9 | 83.6 | 86.7 | 124.4 | 90.2 |
| Run5 | 82.9 | 66.4 | 68.9 | 124.3 | 85.6 |

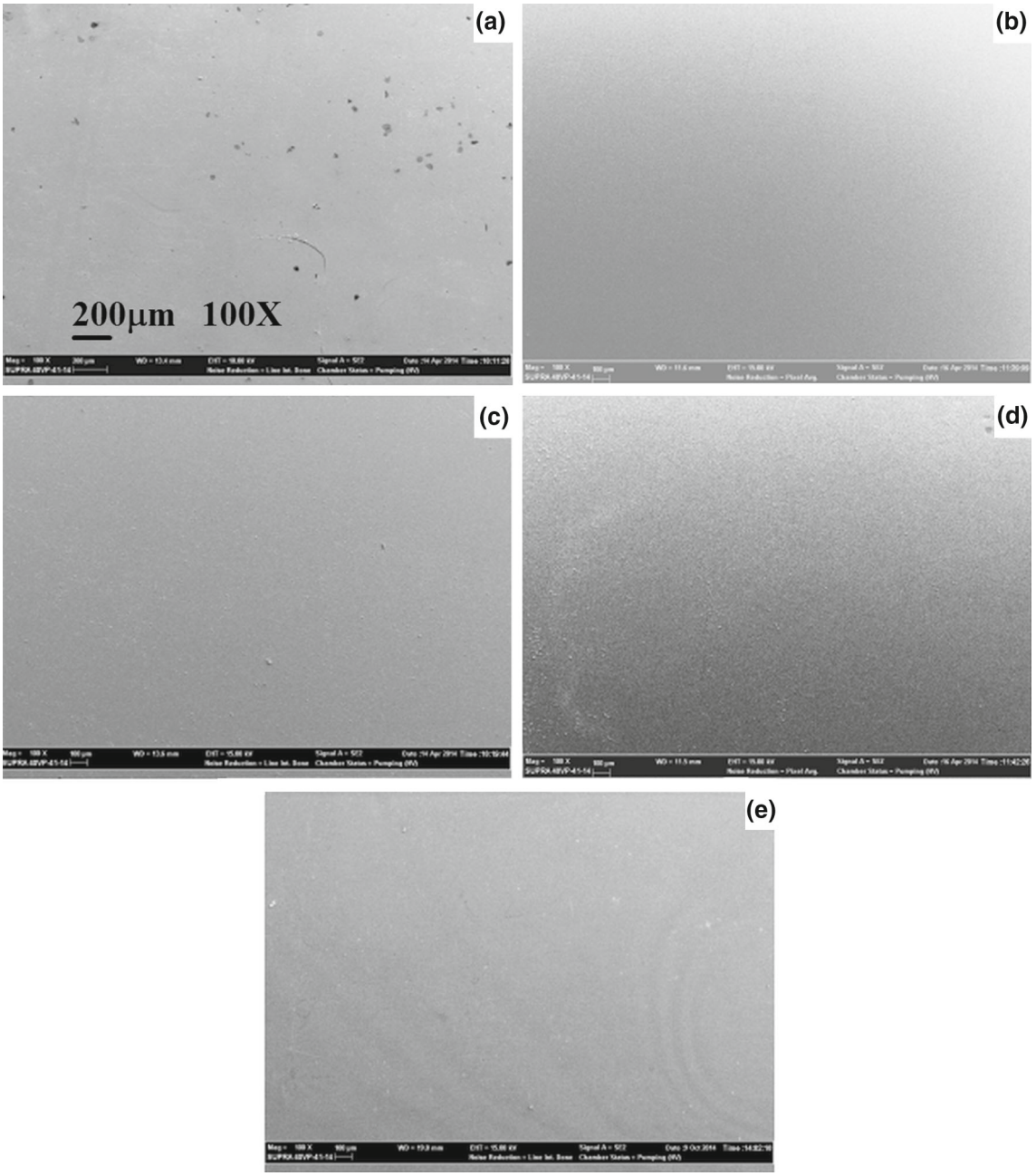


**Fig. 5** Relatively low-magnification (×100) SEM images of a typical top-view of the surface of the PbS thin films obtained in various $Na_2S_2O_3$ concentration of **a** 0 M, **b** 0.0034 M, **c** 0.0068 M, **d** 0.0102 M and **e** 0.0136 M

thin films obtained in run4 and run5 is higher about 20 nm than that of the other films.

The lattice parameter '*a*' was calculated as to be 5.9454 Å which is nearly matched with the reported value of 5.9315 Å.

### 3.3 Surface Morphology of PbS Thin Films

The surface morphology and particle (grain) sizes of the PbS thin films were determined from the SEM images. The accelerating voltage was varied between 10–15 kV for the all SEM images. Figure 5 shows the relatively low-magnification (100×) SEM images of a typical top-view of the surface of the films. It is seen from the Fig. 5a which is the surface image of the film obtained in the absence of the $Na_2S_2O_3$ that there are plenty of pinholes, voids and spots. The surfaces of the other films are very smooth and pinhole free as shown in Fig. 5b–e.

These results are very important since in the latest studies [32–35], various chemicals such as lead acetate ($Pb(CH_3COO)_2{\cdot}3H_2O$), ammonia ($NH_3$), triethanolamine

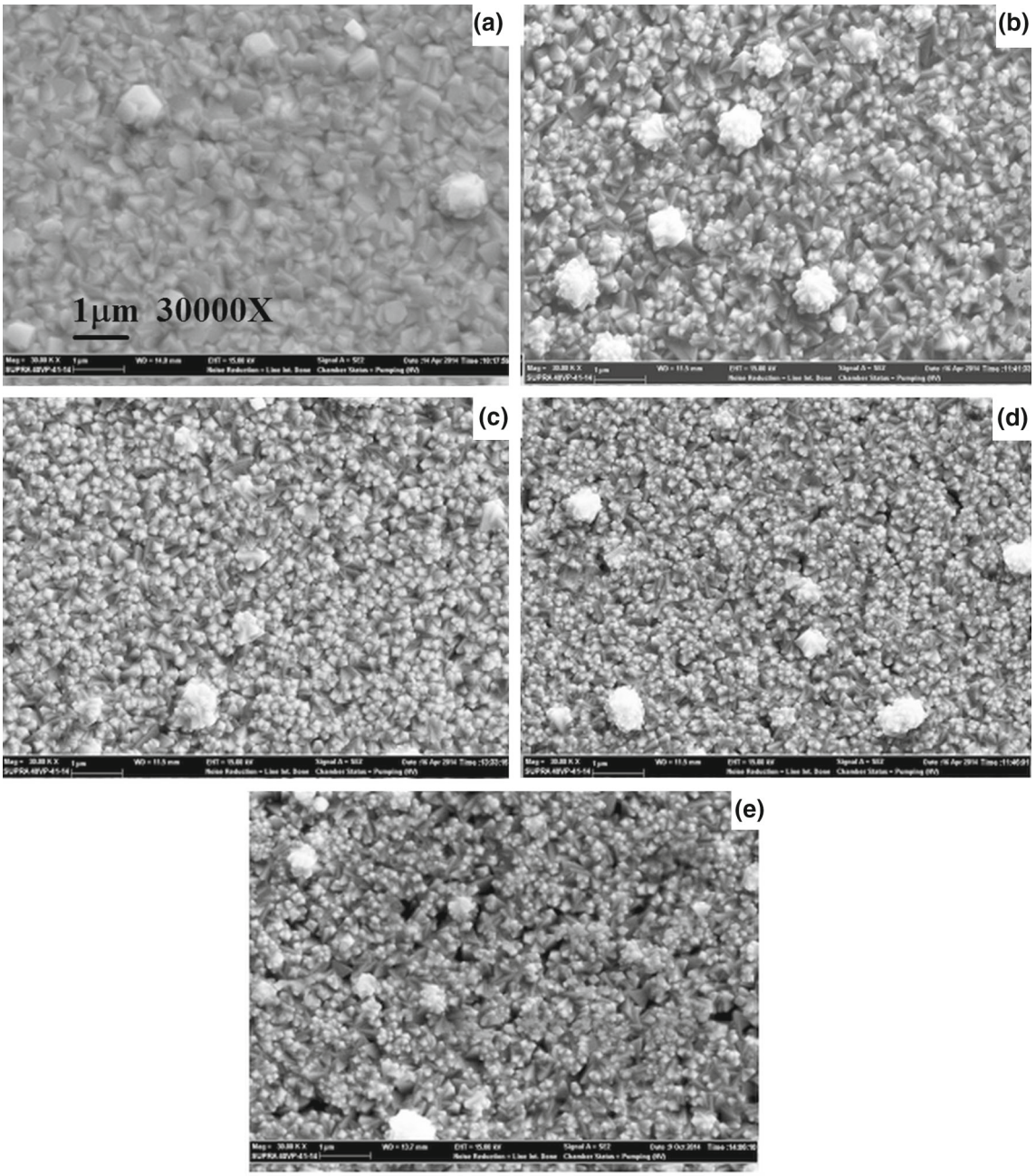


**Fig. 6** Relatively high-magnification (×30,000) SEM images of a typical top-view of the surface of the PbS thin films obtained at various $Na_2S_2O_3$ concentration of **a** 0 M, **b** 0.0034 M, **c** 0.0068 M, **d** 0.0102 M and **e** 0.0136 M

$(N(CH_2CH_2OH)_3)$, thiourea, sodium hydroxide, ethylenediamine $(C_2H_4(NH_2)_2)$, diethanolamine $(HN(CH_2CH_2OH)_2)$ and hexamine $(C_6H_{12}N_4)$ were used for deposition of compact PbS but in these mentioned studies, low-magnification surface images were not obtained and investigated. The relatively higher-magnification (30,000×) surface images of the PbS thin films are shown in Fig. 6. The particles of the film which were obtained in the absence of $Na_2S_2O_3$ formed in polymorphic shape as shown in Fig. 6a and its particle sizes vary between 180 and 590 nm.

When the $Na_2S_2O_3$ was included in the final solutions, the particles changed in shape from the polymorphic form to the pyramidal, which is shown in Fig. 6b–e. The surfaces of the films obtained in run 2 and 3 shown in Fig. 6b, c, respectively, are very uniform and their particle sizes are roughly 215 nm.

## 4 Conclusions

In this study, PbS thin films have been deposited on glass substrates by the CBD. In the traditional method, aqueous solutions of lead nitrate, sodium hydroxide and thiourea are used together for deposition of PbS films [7,12,36,37]. However in this work, sodium thiosulfate was incorporated into these compounds. It was found out from the $Pb^{2+}$ concentrations measurements obtained by AAS that sodium thiosulfate had an inhibitor effect. Thus, chemical kinetics was investigated and the reaction rate constants $k_1$,$k_2$ and reaction order $c$ were calculated as to be 62.5, $-236$ $L^{1.67}$ $min^{-1}$ $mol^{-1.67}$ and 0.36, respectively. The measured $Pb^{2+}$ concentrations were compared with the theoretical ones, and the experimental error ratio was calculated as to be average 10 % for all experiments. Structural analyses were investigated by means of XRD patterns. Using a certain amount of sodium thiosulfate increased peak intensities and crystallization according to the XRD patterns. Surface morphologies of the films were analyzed by using SEM images. When surface image of the film obtained by traditional method magnified 30,000 times, pinholes and voids were not observed. But it magnified only 100 times and then pinholes and voids appeared. This result shows that pinhole and void formation should be researched both relatively low- and high-magnification surface images. However, pinholes and voids formation were completely prevented by using sodium thiosulfate and compact thin films of PbS could be produced. Besides, sodium thiosulfate turned polymorphic particles to the pyramidal form.

## References


1. Hussain, A.; Begum, A.; Rahman, A.: Electrical and optical properties of nanocrystalline lead sulphide thin films prepared by chemical bath deposition. Indian J. Phys. **86**, 697–701 (2012)
2. Obaid, A.S.; Mahdi, M.A.; Hassan, Z.; Bououdina, M.: Characterization of nanocrystalline PbS thin films prepared using microwave-assisted chemical bath deposition. Mater. Sci. Semicond. Process. **15**, 564–571 (2012)
3. Rempel, A.A.; Kozhevnikovab, N.S.; Leenaers, A.J.G.; Vanden Berghe, S.: Towards particle size regulation of chemically deposited lead sulfide (PbS). J. Cryst. Growth **280**, 300–3008 (2005)
4. Tohidi, T.; Jamshidi-Ghaleh, K.; Namdar, A.; Abdi-Ghaleh, R.: Comparative studies on the structural, morphological, optical, and electrical properties of nanocrystalline PbS thin films grown by chemical bath deposition using two different bath compositions. Mater. Sci. Semicond. Process. **25**, 197–206 (2014)
5. Guo, R.F.; Liang, Y.; Gao, X.Y.; Zhu, H.J.; Zhang, S.; Liu, H.T.: Microstructure and near infrared absorption of PbS films deposited by chemical bath deposition on p-Type Si(100) wafers. Braz. J. Phys. **44**, 697–702 (2014)
6. Zaman, S.; Mehmood, S.K.; Mansoor, M.; Asim, M.M.: Effect of lead ion concentration on the structural and optical properties of nano-crystalline PbS thin films. Mater. Sci. Eng. **60**, 012057 (2014)
7. Khot, K.V.; Mali, S.S.; Pawar, N.B.; Mane, R.M.; Kondalkar, V.V.; Ghanwat, V.B.; Patil, P.S.; Hong, C.K.; Kim, J.H.; Heo, J.; Bhosale, P.N.: Novel synthesis of interconnected nanocubic PbS thin films by facile aqueous chemical route. J. Mater. Sci. Mater. Electron. **25**, 3762–3770 (2014)
8. Carrillo-Castillo, A.; Aguirre-Tostado, F.S.; Salasvillasenor, A.; Mejia, I.; Egnade, B.; Sotelo-Lerma, M.; Quevedo-Lopez, M.A.: Effect of chemical bath deposition parameters on the growth of PbS thin films for TFTs applications. Chalcogenide Lett. **10**, 105–111 (2013)
9. Obaid, A.S.; Mahdi, M.A.; Hassan, Z.; Bououdina, M.: PbS nanocrystal solar cells fabricated using microwave-assisted chemical bath deposition. Int. J. Hydrog. Energy **38**, 807–815 (2013)
10. Raniero, L.; Ferreira, C.L.; Cruz, L.R.; Pinto, A.L.; Alves, R.M.P.: Photoconductivity activation in PbS thin films grown at room temperature by chemical bath deposition. Phys. B **405**, 1283–1286 (2010)
11. Hussain, A.; Begum, A.; Rahman, A.: Characterization of nanocrystalline lead sulphide thin films prepared by chemical bath deposition technique. Arab. J. Sci. Eng. **38**, 169–174 (2013)
12. Saravana Kumaran, T.; Parveen Banu, S.: Investigation on structural and optical properties of chemically deposited PbS thin films. Int. J. Recent Sci. Res. **4**, 1685–1687 (2013)
13. Soonmin, H.; Kassim, A.; Weetee, T.: The role of bath temperature in aqueous acidic chemically PbS films. J. Basic Appl. Sci. Res. **3**(11), 353–357 (2013)
14. Soonmin, H.; Kassim, A.; Weetee, T.: Chemical bath deposited lead sulphide thin films: preparation and characterization . World Mech. **1**, 1–6 (2014)
15. Gadave, K.M.; Jodgudri, S.A.; Lokhande, C.D.: Chemical deposition of PbS from an acidic bath. Thin Solid Films **245**, 7–9 (1994)
16. Ayata, S.; Yıldıran, H.: A novel technique for silver extraction from silver sulphide ore. Turk. J. Chem. **25**, 187–191 (2001)
17. Altıokka, B.; Baykul, M.C.; Altıokka, M.R.: Some physical effects of reaction rate on PbS thin films obtained by chemical bath deposition. J. Cryst. Growth **384**, 50–54 (2013)
18. Lisco, F.; Abbas, A.; Maniscalco, B.; Kaminski, P.M.; Losurdo, M.; Bass, K.; Claudio, G.; Walls, J.M.: Pinhole free thin film CdS deposited by chemical bath using a substrate reactive plasma treatment. J. Renew. Sustain. Energy **6**, 011202 (2014)
19. Osherov, A.; Golan, Y.: Chemical solution deposited PbS thin films on Si(100). Phys. Status Solidi C Curr. Top. Solid State Phys. **11**, 3431–3436 (2008)
20. Belova, N.S.; Uritskaya, A.A.; Kitaev, G.A.: Kinetics of lead sulfide precipitation from citrate solutions of thiourea. Russ. J. Appl. Chem. **75**, 1562–1565 (2002)
21. Choudhury, N.; Sarma, B.K.: Structural characterization of lead sulfide thin films by means of X-ray line profile analysis. Bull. Mater. Sci. **32**, 43–47 (2009)
22. Narayanan, K.L.; Viljayakumar, K.P.; Nair, K.G.M.; Rao, G.V.N.: Chemical bath deposition of CdS thin films and their partial conversion to CdO on annealing. Bull. Mater. Sci. **20**, 287–295 (1997)
23. Oliva, A.I.; Corona, J.E.; Patino, R.; Oliva-Aviles, A.I.: Chemical bath deposition of CdS thin films doped with Zn and Cu. Bull. Mater. Sci. **37**, 247–255 (2014)
24. Mochahari, P.K.; Sarma, K.C.: X-ray diffraction line profile analysis of polyvinyl alcohol capped cadmium sulphide nanostructured films. Indian J. Phys. **88**, 1265–1270 (2014)
25. Bruno Chandrasekar, L.; Vijayalakshmi, R.; Rajeswari, B.; Chandramohan, R.; Arivazhagan, G.; Arulmozhi Packiaseeli, S.: Preparation and characterization of silver selenide thin film. Braz. J. Phys. **44**, 653–657 (2014)
26. Qian, N.; Zhang, L.; Ma, W.; Zhao, X.; Han, L.; Lu, W.: Core–shell $Al_2O_3$-supported Ni for high-performance catalytic reforming of toluene as a model compound of tar. Arab. J. Sci. Eng. **39**, 6671–6678 (2014)

27. Begum, A.; Hussain, A.; Rahman, A.: Structural and optical studies of bismuth sulphide nanocrystalline thin films prepared from acidic aqueous bath. Arab. J. Sci. Eng. **38**, 163–168 (2013)
28. Ali, M.; Basu, P.; Liwa, M.; Fadhel, M.I.; Souiyah, M.; Ziend, B.A.: Comparison between the properties of Al–TiC and Al–(TiC + $Fe_3C$ + $Fe_2Ti$ + Fe) composites. Arab. J. Sci. Eng. **38**, 2785–2791 (2013)
29. Lebid, M.; Omari, M.: Synthesis and electrochemical properties of $LaFeO_3$ oxides prepared via sol–gel method. Arab. J. Sci. Eng. **39**, 147–152 (2014)
30. Bedir, M.; Öztaş, M.; Korkmaz, D.; Özdemir, Y.: Influence of preparation conditions on the dispersion parameters of sprayed $In_2S_3$ films. Arab. J. Sci. Eng. **39**, 503–509 (2014)
31. Nalbant, A.; Ertek, Ö.; Okur, I.: The structural properties of ZnO thin films produced in different molarities by spin coating method. Arab. J. Sci. Eng. **38**, 1909–1915 (2013)
32. Navale, S.T.; Bandgar, D.K.; Chougule, M.A.; Patil, V.B.: Facile method of preparation of PbS films for $NO_2$ detection. R. Soc. Chem. **5**, 6518–6527 (2015)
33. Fan, L.; Wang, P.; Guo, Q.; Han, H.; Li, M.; Chen, Z.; Zhao, H.; Zhang, D.; Zheng, Z.; Yung, J.: Ultrasound-modulated microstructure of PbS film in ammonia-free chemical bath deposition. R. Soc. Chem. **5**, 10018–10025 (2015)
34. Chen, Y.; Zhang, X.; Tao, Q.; Fu, W.; Yang, H.; Su, S.; Mu, Y.; Zhou, L.; Li, M.: High catalytic activity of a PbS counter electrode prepared via chemical bath deposition for quantum dots-sensitized solar cells. R. Soc. Chem. **5**, 1835–1840 (2015)
35. Carrillo-Castillo, A.; Ambrosio Lázaro, R.C.; Jimenez-Pérez, A.; Martínez Pérez, C.A.; Cruz Terrazas, E.C.de la ; Quevedo-López, M.A.: Role of complexing agents in chemical bath deposition of lead sulfide thin films. Mater. Lett. Chem. **121**, 19–21 (2014)
36. Touati, B.; Gassoumi, A.; Alfaify, S.; Kamoun-Turki, N.: Optical, morphological and electrical studies of Zn:PbS thin films. Mater. Sci. Semicond. Process. **34**, 82–87 (2015)
37. Yang, J.; Walker, A.V.: Morphological control of PbS grown on functionalized self-assembled monolayers by chemical bath deposition. Langmuir **30**, 6954–6962 (2014)